JOURNAL OF VIROLOGY, Jan. 2006, p. 210–217 Vol. 80, No. 1
0022-538X/06/$08.00+0 doi:10.1128/JVI.80.1.210–217.2006

Severe Acute Respiratory Syndrome Coronavirus 3a Protein Is Released in Membranous Structures from 3a Protein-Expressing Cells and Infected Cells

Cheng Huang,[1]† Krishna Narayanan,[1]† Naoto Ito,[1,2] C. J. Peters,[1,3] and Shinji Makino[1]*

Department of Microbiology and Immunology[1] and Department of Pathology,[3] The University of Texas Medical Branch at Galveston, Galveston, Texas 77555-1019, and Laboratory of Zoonotic Diseases, Division of Veterinary Medicine, Faculty of Applied Biological Science, Gifu University, 1-1 Yanagido, Gifu 501-1193, Japan[2]

Received 11 July 2005/Accepted 3 October 2005

Severe acute respiratory syndrome coronavirus (SCoV) accessory protein 3a is a virus structural protein. We demonstrate here that 3a protein was released efficiently in membranous structures from various cell lines expressing 3a protein. A subpopulation of the released 3a protein is associated with detergent-resistant membranes. The presence of the YxxΦ and diacidic motifs, located within the cytoplasmic tail of the 3a protein, was not required for its efficient release. Analysis of supernatant from SCoV-infected cells with sucrose gradient sedimentation and virus capture assay indicated that the 3a protein was released from infected cells in two distinct populations, as a component of SCoV particles, and in membrane structures with a lower buoyant density. These data provide new insights into the biological properties of SCoV 3a protein.

Severe acute respiratory syndrome (SARS) coronavirus (SCoV), an enveloped, single-stranded, and positive-sense RNA virus, is the etiological agent of a new human disease, SARS (10, 18, 19, 22, 36). During SCoV replication, viral genomic-sized RNA plus eight subgenomic mRNAs are produced (26, 40, 49). These subgenomic mRNAs encode the spike glycoprotein (S), M glycoprotein (M), nucleocapsid protein (N), and E protein (E), all of which are the viral structural proteins found in all coronaviruses (20). In addition, some subgenomic mRNAs are predicted to encode several SCoV-specific accessory proteins (49). Although other coronaviruses also encode accessory proteins, there are no significant similarities in the amino acid sequences among these coronavirus accessory proteins and any known cellular or viral proteins. Two SCoV accessory proteins, 3a and 7a proteins, have been shown to be expressed in SCoV-infected cells (12, 17, 30, 47, 55, 57). Past studies have suggested that coronavirus accessory proteins are generally not essential for virus replication in cell culture, and yet they may play roles in viral pathogenesis in vivo (9, 34, 35, 52, 53). It has been reported that apoptosis is induced in the cells expressing SCoV 7a protein (45) and those expressing SCoV 3a protein (21).

The SCoV 3a protein, consisting of 274 amino acids, is one of the viral structural proteins that is expressed abundantly in infected cells (17, 43). SCoV 3a protein has been detected in a lung specimen from a SCoV-infected patient (55), and antibodies to 3a protein are detected in convalescent SARS patients (46). In infected cells, 3a protein is localized in intracellular and plasma membranes and is also found in association with intracellular SCoV particles (17, 55, 56). SCoV 3a protein appears to be an integral membrane protein and contains two intracellular protein sorting and trafficking signals, the YxxΦ and diacidic motifs, in the C terminus. SCoV 3a protein deletion mutant lacking a region encompassing both motifs fails to transport to the cell surface (47). It has been proposed that 3a protein might be incorporated into virus particles by direct association with S protein in infected cells (57). Indeed, 3a protein interacts with S and M proteins, in the Golgi apparatus (47, 55), where virus assembly and budding occurs (14, 39, 50). However, in the absence of S protein, 3a protein is still capable of being incorporated into virus-like particles (VLPs) in cells expressing SCoV M, E, and 3a proteins (43). Thus, like the S protein of coronaviruses, 3a protein is dispensable for VLP formation (15, 16, 27), whereas it can be incorporated into virus particles through its interaction with other SCoV envelope proteins, e.g., S and/or M proteins. Biological functions of 3a protein in SCoV particles and infected cells are unclear.

In the present study we demonstrated that the expression of 3a protein alone in cultured cells resulted in the release of 3a protein in membranous structures. Furthermore, analysis of culture supernatant from SCoV-infected cells indicated that the 3a protein-containing membranous structures were also released from infected cells.

MATERIALS AND METHODS

Cells and virus. Human embryonic kidney 293T cells and Vero E6 cells were maintained in Dulbecco modified Eagle medium supplemented with 10% fetal bovine serum, L-glutamine (2 mM), nonessential amino acids (0.1 mM), and kanamycin (100 μg/ml). Human colon carcinoma epithelium CaCo-2 cells were maintained in Minimum essential medium (Eagle) with 20% fetal bovine serum, L-glutamine (2 mM), nonessential amino acids (0.1 mM), and kanamycin (100 μg/ml). Cells were incubated at 37°C in 5% CO_2. The Urbani strain of SCoV was grown as described previously (17, 28).

Construction of plasmids for transient expression. Total intracellular RNA was extracted from SCoV-infected Vero E6 cells with TRIzol reagent (Invitrogen) according to the manufacturer's protocol. SCoV 3a and 7a genes were amplified from total RNA prepared from SCoV-infected cells by reverse tran-

* Corresponding author. Mailing address: Department of Microbiology and Immunology, The University of Texas Medical Branch at Galveston, Galveston, TX 77555-1019. Phone: (409) 772-2323. Fax: (409) 772-5065. E-mail: shmakino@utmb.edu.

† C.H. and K.N. contributed equally to this study.

scription-PCR. The PCR products were cloned into a mammalian expression vector pCAGGS (kindly provided by Yoshihiro Kawaoka, University of Tokyo, Tokyo, Japan), resulting in pCAGGS-3a and pCAGGS-7a, respectively. A mutant 3a gene, containing deletion mutations in the YxxΦ and diacidic motif (160 to 173 amino acids [aa]), was constructed by using two-step recombinant PCR. The PCR product was inserted into pCAGGS, yielding pCAGGS-3aΔ. The pCAGGS-3aYA, pCAGGS-3aAA, and pCAGGS-3aA3 mutants were constructed by using a QuikChange II site-directed mutagenesis kit (Stratagene). The sequences of the constructed plasmids were confirmed by sequence analyses.

Transient protein expression. 293T cells grown on 10-cm plates were transfected with pCAGGS-3a or other plasmids, as indicated in each experiment, by using TransIT-293 reagent (Mirus, Madison, WI) according to the manufacturer's instructions. At different times after transfection, as indicated, culture media were removed and cells were washed once with phosphate-buffered saline. Total cell lysates were prepared by using 1× sodium dodecyl sulfate-polyacrylamide gel electrophoresis (SDS-PAGE) loading buffer (62.5 mM Tris-HCl [pH 6.8], 2% SDS, 10% glycerol, 50 mM dithiothreitol), and the samples were boiled for 5 min.

Preparation of antibodies and Western blotting. Methods for preparation of rabbit anti-3a polyclonal antibody were reported previously (17). Anti-SCoV 7a protein antibody was developed by immunizing rabbits with synthetic peptide N-PSGTYEGNSPFH, corresponding to aa 35 to 46 of SARS 7a protein, and was affinity purified by the synthetic peptide. Rabbit anti-SCoV S polyclonal antibody (IGM-541) was obtained from IMGENEX, San Diego, CA. Rabbit anti-SCoV M antibody (AP6008b) was purchased from Abgent, San Diego, CA. Mouse anti-SCoV N antiserum was provided by Xiao-Hua Li at University of Texas Southwestern Medical Center at Dallas. Mouse monoclonal anti-SCoV S protein antibody, NR-617, was obtained through the NIH Biodefense and Emerging Infections Research Resources Repository, National Institute of Allergy and Infectious Disease. Goat anti-actin antibody, horseradish peroxidase (HRP)-conjugated goat anti-rabbit immunoglobulin G (IgG), HRP-conjugated goat anti-mouse IgG, and HRP-conjugated donkey anti-goat IgG were purchased from Santa Cruz Biotechnology, Santa Cruz, CA. Western blotting was performed as described previously (17). Briefly, protein samples were separated by SDS-PAGE and transferred onto polyvinylidene difluoride membranes (Bio-Rad) with the Trans-Blot SD semidry transfer apparatus (Bio-Rad). The membranes were blotted with primary antibodies overnight at 4°C and subjected to incubation with secondary antibodies for 1 h at room temperature. The protein bands were visualized with ECL reagent (Amersham Biosciences) according to the manufacturer's instructions.

Purification of 3a-containing membrane structures and SCoV. At 48 h after transfection, culture supernatants were harvested and centrifuged at 1,500 × *g* for 10 min at 4°C to remove cell debris. Samples were further clarified by filtration through 0.45-μm-pore-size syringe filters. 3a-containing membrane structures were then pelleted by centrifugation through a 20% sucrose cushion at 26,000 rpm for 3 h at 4°C by using a Beckman SW28 rotor. To determine the buoyant density of the 3a-containing membranous structures released from expressing cells, the vesicles that were pelleted through a 20% sucrose cushion were suspended in NTE buffer (100 mM NaCl, 10 mM Tris-HCl [pH 7.5], 1 mM EDTA), applied onto a 20 to 60% continuous sucrose gradient, and subjected to centrifugation at 26,000 rpm for 18 h on an SW28 rotor. Twelve fractions were collected from the bottom of the gradient. After the densities of each fraction were measured, they were then diluted with NTE buffer and centrifuged through 20% sucrose as described above. The pellets were dissolved in 1× SDS-PAGE loading buffer and used for Western blot analysis. For purification of 3a-containing membranous structures from SCoV-infected cells, supernatants from SCoV-infected Caco2 cells were inactivated by irradiation with 2×10^6 rads by a Gammacell ^{60}Co source (model 109A; JL Shepherd and Associates, San Fernando, CA) as described previously (17). The inactivation of virus infectivity was confirmed by tissue culture assay. After centrifugation at 1500 × *g* for 10 min at 4°C, samples were further clarified by filtration through 0.45-μm-pore-size syringe filters. The clarified samples were partially purified by centrifugation through 20% sucrose cushions, resuspended in NTE buffer, and then applied onto a 20 to 60% continuous sucrose gradient and subjected to centrifugation at 26,000 rpm for 18 h by using a Beckman SW28 rotor. Twelve fractions were collected and diluted in NTE. SCoV virions and 3a-containing membrane structures were pelleted through a 20% sucrose cushion as described above.

Membrane flotation assay. Purified 3a-containing pellets were suspended in NTE buffer. In some experiments, 3a-containing pellets were suspended in NTE buffer containing 1% Triton X-100 and incubated at room temperature or 4°C for 30 min, as indicated. Sucrose was then added to the suspension to adjust the final concentration to 60% (wt/wt). The samples were transferred to the bottom of Beckman SW41 centrifuge tubes and overlaid with 50% sucrose and 10% sucrose. The samples were then centrifuged to equilibrium at 38,000 rpm for 18 h by using a Beckman SW41 rotor. Fractions were collected from the top to the bottom of the gradient. Equal amounts of each fraction were diluted in NTE buffer and analyzed by Western blotting.

SCoV virus capture assay. SCoV virus capture assay was performed by using the methods described by others with modifications (31). Supernatants from SCoV-infected Caco2 cells were centrifuged at 1,500 × *g* for 10 min at 4°C to remove cell debris. The supernatants were then applied to top of the 20% sucrose cushion, and the samples were centrifuged at 26,000 rpm for 3 h at 4°C by using a Beckman SW28 rotor. The pellet was suspended in NTE buffer containing 0.3% of bovine serum albumin, proteinase inhibitor cocktail (Sigma), and protein A-Sepharose 4 Fast Flow beads (Amersham Biosciences) and then incubated at 4°C for 1 h. After centrifugation at 750 × *g* for 5 min, the supernatant was collected and then mixed with 5 μg of mouse anti-SCoV S protein monoclonal antibody, NR-167, or mouse anti-H2K^{K}D^K (H2K) monoclonal antibody (29). After incubation at 4°C overnight, 5 μg of goat anti-mouse IgG (Fcγ fragment specific; Jackson Immunoresearch Laboratories, Inc., West Grove, PA) was added to the samples. After incubation at 4°C for 3 h, protein A-Sepharose Fast Flow beads were added to the samples, followed by further incubation for another 3 h at 4°C. After centrifugation at 750 × *g* for 5 min, the supernatant was collected. The pellets were suspended in NTE buffer and then washed with NTE buffer five times. Finally, the collected supernatant and the pellets were suspended in SDS-PAGE loading buffer and used for SDS-PAGE and subsequent Western blot analysis.

RESULTS

SCoV 3a protein is released from 3a-expressing cells. To examine whether expression of 3a alone results in release of 3a protein into culture supernatant, 293T cells were transfected with pCAGGS-3a, in which the entire 3a gene was cloned downstream of a chicken β-actin promoter of pCAGGS. As a control, the parental pCAGGS plasmid was used for transfection. Western blot analysis, using anti-3a antibody, showed expression of 3a protein in pCAGGS-3a-transfected cells, whereas no 3a protein was detected in the control sample (Fig. 1A). Several 3a-related signals with molecular masses from 15 to 37 kDa were detected; in all experiments, 3a protein of 37 kDa (designated 3a-1 in the present study) appeared as a major 3a protein signal. 3a protein of 31 kDa (designed 3a-2) was consistently detected in the 3a protein transient-expression experiments, whereas the abundance of this protein varied among experiments (data not shown). To examine whether the expressed 3a protein could be released into culture medium, clarified culture supernatants from 3a-expressing and control cells were applied to the top of a 20% sucrose cushion, and the samples were centrifuged at 26,000 rpm for 3 h at 4°C by using a Beckman SW28 rotor. Western blot analysis of the pellet with anti-3a antibody clearly demonstrated that 3a-1 was released into the culture media of 3a-expressing 293T cells (Fig. 1A). Densitometry analysis showed that the amount of released 3a-1 in culture medium was ca. 8% of the corresponding intracellular 3a-1 protein signal. As shown in some experiments (see Fig. 2A and 3), 3a-2 was also readily detected in culture medium. Analysis of the supernatants from 3a-expressing Vero E6 cells and Caco2 cells also revealed the release of 3a protein into culture media (data not shown), which demonstrated that the release of 3a protein from the expressing cells was not dependent on cell type. In contrast to 3a protein, another SCoV accessory protein, 7a protein, was not released into culture medium from 7a-expressing 293T cells (Fig. 1B). Also, actin, an abundant host protein, was not found in the supernatants from both 3a- and 7a-expressing 293T cells, strongly suggesting that the presence of 3a protein in the cul-

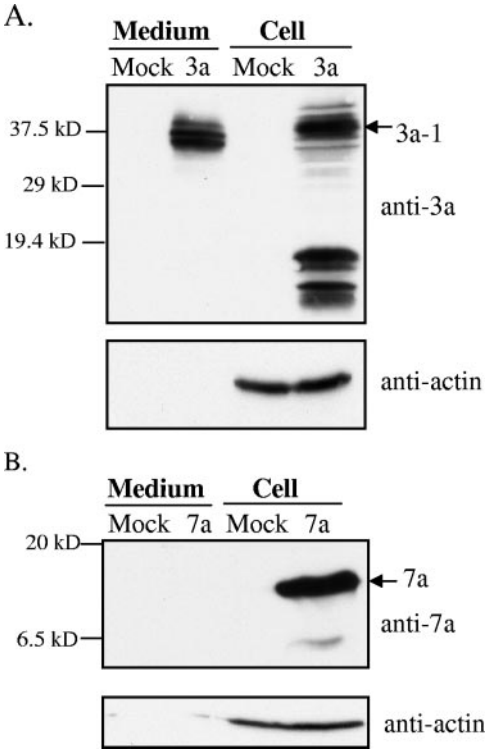

FIG. 1. Release of SCoV 3a protein from 3a protein-expressing cells. 293T cells were independently transfected with pCAGGS (mock), pCAGGS-3a (3a), or pCAGGS-7a (7a). After 48 h transfection, supernatants from transfected cells were clarified, applied onto a 20% sucrose cushion, and centrifuged at 26,000 rpm for 3 h at 4°C. The pellets were suspended in 1× SDS-PAGE loading buffer (Medium). Cell lysates were prepared with 1× SDS-PAGE loading buffer (Cell). Samples were subjected to Western blotting analysis with anti-3a antibody (A) and anti-7a antibody (B). The membranes were reprobed with anti-actin antibody (anti-actin). 3a-1 indicates 3a protein with a molecular mass of ~37 kDa.

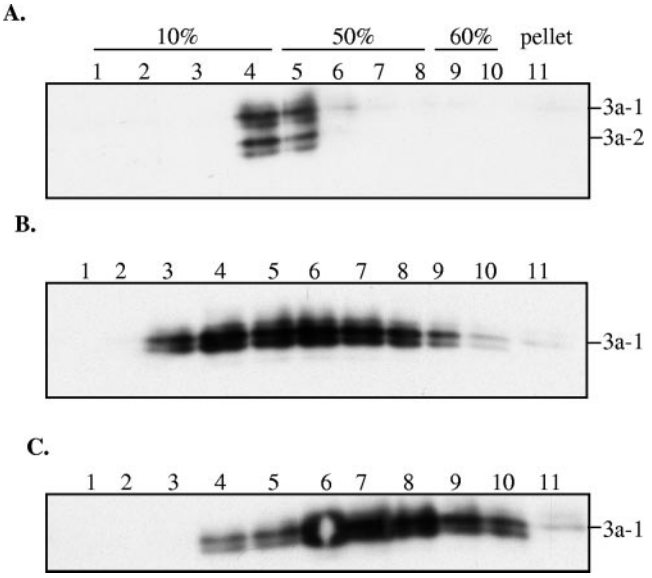

FIG. 2. Flotation assay of 3a-containing membranous structures. Purified 3a-containing membrane structures from the media of 3a-expressing 293T cells were suspended in NTE buffer (A), in NTE buffer containing 1% Triton X-100 and incubated at 4°C for 30 min (B), or in NTE buffer containing 1% Triton X-100 at room temperature and incubated for 30 min (C). After sucrose was added to adjust the final concentration to 60%, the samples were transferred to the bottom of Beckman SW41 centrifuge tubes and overlaid with 50% sucrose and 10% sucrose. The step gradient was centrifuged to equilibrium at 38,000 rpm for 18 h by using a Beckman SW41 rotor. Fractions were collected from top to bottom. Equal amounts of each fraction were diluted in NTE buffer, separated by SDS-PAGE, and analyzed by Western blotting with anti-3a antibody. 3a-1 and 3a-2 indicate the slow-migrating (37 kDa) and fast-migrating (31 kDa) forms of the 3a protein, respectively.

ture media of 3a-expressing cells was not simply due to the leaking of intracellular proteins or contamination of cell debris in the prepared samples.

Characterization of membranous structures carrying 3a protein. Both topological prediction and biochemical studies have suggested that 3a is an integral membrane protein with three membrane-spanning regions (47, 55, 56). A membrane flotation assay showed the migration of the released 3a protein from the bottom of the gradient, containing 60% sucrose, to the interface of 10 to 50% sucrose (Fig. 2A), demonstrating that 3a protein was released in association with membranous structures. When the pellet containing 3a-containing membrane structures was treated with 1% Triton X-100 at 4°C prior to flotation assay, a significant portion of 3a protein was present in the interface of 10 to 50% sucrose (fractions 4, 5, and 6, Fig. 2B), and only a low level of 3a protein was detected in the bottom of the gradient (fractions 10 and 11 and pellet, Fig. 2B). A similar result was observed when the pellet carrying 3a protein was treated with 1% NP-40 at 4°C (data not shown). When the pellet containing 3a-containing membrane structures was treated with 1% Triton X-100 at room temperature and monitored by a membrane flotation assay, the majority of 3a-containing membrane structures was found at the bottom of the gradient, but a small population of 3a protein was still detectable in the interface of 10 to 50% sucrose (Fig. 2C). These results indicated that at least some of the 3a protein in the membrane structures was resistant to detergent treatment, strongly suggesting that a subpopulation of the released 3a protein is associated with detergent-resistant membranes (5, 7, 37).

Sucrose density equilibrium ultracentrifugation of the 3a-containing membranous structures showed that 3a protein displayed a relatively broad distribution in the gradient, ranging from 1.21 to 1.11 g/ml (Fig. 3, fractions 4 to 10), and the peak signal of 3a protein was observed at about 1.14 to 1.16 g/ml (Fig. 3, fractions 7 and 8), which was lighter than the buoyant densities (1.160 to 1.185 g/ml) of SCoV (17).

Release of 3a protein from SCoV-infected cells. We next tested whether 3a-containing membranous structures were produced in SCoV-infected cells. We previously had analyzed a highly purified SCoV sample and did not observe the presence of 3a-containing membranous structures with a lighter buoyant density than SCoV (17). In that experiment, SCoV was purified by two successive discontinuous sucrose gradient centrifugations, for 3 and 18 h, and a continuous overnight sucrose gradient centrifugation. Although this purification procedure is suitable for SCoV purification, it might have excluded putative 3a-containing membranous structures during

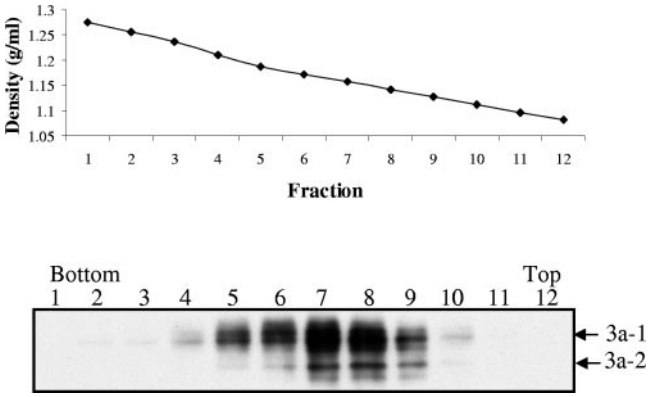

FIG. 3. Analysis of the buoyant density of 3a-containing membrane structures. The supernatant of 3a-expressing 293T cells was collected at 48 h after transfection and partially purified by centrifugation on a 20% sucrose cushion. The pellets were suspended in NTE buffer, loaded on a 20 to 60% continuous sucrose gradient, and centrifuged at 26,000 rpm for 18 h using an SW28 rotor. Twelve fractions were taken from the bottom, and the densities of each action were measured (upper panel). Each fraction was then diluted at least threefold with NTE buffer and was then centrifuged on a 20% sucrose cushion. The recovered pellets were suspended in 1× SDS-PAGE loading buffer and subjected to Western blotting analysis with anti-3a antibody (lower panel).

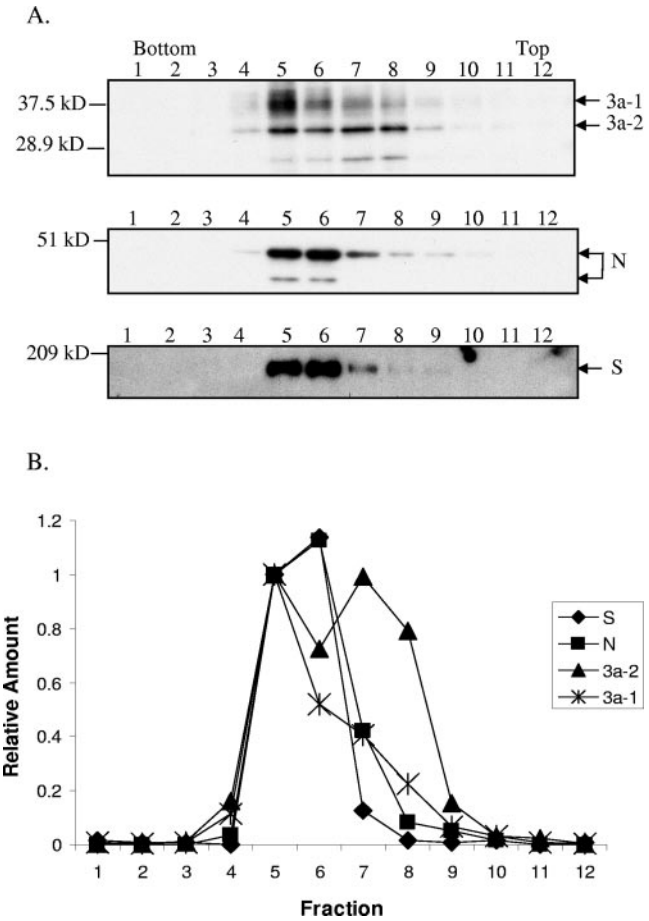

FIG. 4. Release of 3a protein from SCoV-infected cells. (A) Supernatants from SCoV-infected Caco2 cells were harvested and inactivated by irradiation. The samples were clarified and partially purified by centrifugation on a 20% sucrose cushion. SCoV virions were suspended in NTE buffer, loaded on continuous 20 to 60% sucrose gradient, and centrifuged at 26,000 rpm for 18 h by using a Beckman SW28 rotor. Twelve fractions were taken from the bottom, and each was then diluted at least three times with NTE buffer, followed by centrifugation on 20% sucrose cushion. The recovered virus samples were dissolved in 1× SDS-PAGE loading buffer and detected by Western blotting with anti-3a antibody, anti-SCoV N protein antibody, and anti-SCoV S protein antibody, as indicated. 3a-1 and 3a-2 indicate the slow-migrating form (37 kDa) and fast-migrating form (31 kDa) of 3a protein, respectively. (B) The 3a, N, and S protein levels were measured by densitometry analysis with AlphaEase software (Alpha Innotech). For each protein, the level of protein in fraction 5 was arbitrarily set as 1. The relative amounts of each protein in different fractions are shown.

the purification steps. In the present study, supernatants from SCoV-infected Caco2 cells were clarified by low-speed centrifugation and subsequent filtration. The released SCoV and putative membrane-structures containing 3a protein were pelleted by ultracentrifugation through a 20% sucrose cushion and then applied onto a 20 to 60% continuous sucrose gradient for subsequent ultracentrifugation for 18 h. Western blot analysis of each sucrose fraction (Fig. 4A) and their densitometric scans (Fig. 4B) showed that the peak signals of N and S proteins were in fractions 5 and 6, corresponding to the densities of 1.20 and 1.18 g/ml, respectively (Fig. 4A), which indicated that the buoyant density of SCoV was about 1.18 to 1.20 g/ml, similar to that previously reported (15–17). The 3a-1 signal tracked closely with the virus peak. However, the 3a-2 concentration was high in all of the fractions from 5 to 8, corresponding to the virion density of 1.18 to 1.20 g/ml and less-dense fractions of 1.13 to 1.15 g/ml. We repeated these studies three times with similar results. These findings, combined with the detergent fractionation results, support the idea that significant quantities of 3a in the form of 3a-2 (31 kDa) are present as extracellular membrane structures. In contrast, most of the 3a-1 (37 kDa) is associated with the virion fractions.

To further demonstrate release of the 3a-containing membranous structures from SCoV-infected cells, we conducted the virus capture assay, in which anti-SCoV S protein antibody was used to immunoprecipitate the intact SCoV particles from culture supernatant from infected cells. If SCoV particles primarily incorporate 3a-1 (Fig. 4), then the largest 3a-1 signal would be detected in the immunoprecipitated sample. Because it appeared that the putative 3a-containing membranous structures contained predominantly 3a-2, with a low level of 3a-1 and did not have S protein (Fig. 4), we expected that anti-S protein antibody would not immunoprecipitate the 3a-containing membrane structures, and 3a-2 would be detected primarily in unprecipitated samples. The 3a-2 signal was slightly stronger than the 3a-1 signal in the sample that was pelleted down from the supernatant of SCoV-infected cells through a 20% sucrose cushion (Fig. 5A, lane 1). As expected, a nonspecific monoclonal mouse anti-H2K antibody failed to immunoprecipitate any 3a protein signals (Fig. 5A, lane 2). The sample that was immunoprecipitated by a mouse monoclonal anti-SCoV S protein antibody contained predominantly a 3a-1 signal with a low level of 3a-2 signal (Fig. 5A, lane 3), strongly suggesting the efficient incorporation of 3a-1 signal into SCoV particles. In contrast, the 3a-2 signal was clearly stronger than

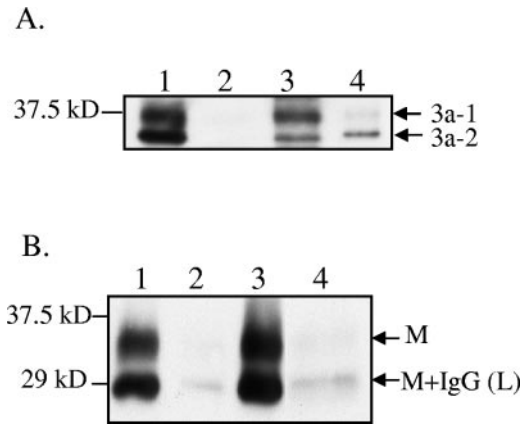

FIG. 5. SCoV capture assay. Clarified supernatants from SCoV-infected Caco2 cells were applied to the top of the 20% sucrose cushion, and then the samples were centrifuged at 26,000 rpm for 3 h at 4°C by using a Beckman SW28 rotor. Lane 1 represents the pellet fraction. The suspended pellets were immunoprecipitated by nonspecific monoclonal mouse anti-H-2K antibody (lane 2) or by a mouse monoclonal anti-SCoV S antibody to capture virions (lane 3). Lane 4 represents supernatant that was not precipitated by anti-SCoV S antibody. All of the samples were examined with a rabbit anti-SCoV 3a antibody (A) and a rabbit anti-SCoV M antibody (B) in Western blot analysis.

the 3a-1 signal in the sample that was not immunoprecipitated with this anti-S protein antibody (Fig. 5A, lane 4), and the pattern of 3a protein signals in this sample was similar to that of 3a protein signals in fractions 7 and 8 shown in Fig. 4. In a control analysis, M protein was detected in the sample that was immunoprecipitated by a monoclonal anti-SCoV S protein antibody and not in the sample immunoprecipitated with anti-H2K antibody (Fig. 5B). A minor signal that was detected in the sample immunoprecipitated with anti-H2K antibody and the unprecipitated sample represented the IgG light chain. These control experiments confirmed the specificity of the virus capture assay, which showed that 3a-1 protein was preferentially associated with virus particles and smaller amounts of the 3a-2 protein were associated with SCoV particles; conversely, the material not precipitated with anti-S contained primarily 3a-2 with small amounts of 3a-1. The concordance of the results from these two different experimental approaches (ultracentrifugation and immunoprecipitation) strongly suggests that membrane structures predominantly containing 3a-2 are released from SCoV-infected cells.

Role of YxxΦ and diacidic motifs in the release of 3a protein. 3a protein contains two intracellular protein sorting and trafficking motifs, the YxxΦ motif and diacidic motif, in its cytoplasmic tail (Fig. 6A). It was previously reported that when a 14-amino-acid region containing these motifs was deleted, 3a protein fails to transport to the cell surface (47). The juxtaposition of these two motifs, as well as their proximity to the third putative transmembrane region, suggests they might participate in the intracellular transport of 3a protein. To investigate the possible role of these motifs in the release of 3a protein, we first constructed a plasmid vector, pCAGGS-3aΔ, expressing a 3a protein deletion mutant (3aΔ protein) that lacked the 14-aa domain (aa 160 to 173) containing the YxxΦ and diacidic motifs (Fig. 6A). The deletion site of the 3aΔ protein was the same as the deletion region of a previously characterized 3a deletion mutant that no longer translocated onto the cell surface (47). As shown in Fig. 6B, only a trace level of 3aΔ protein was detected in the culture medium of transfected 293T cells, whereas the intracellular expression level of the 3aΔ protein in these cells was only slightly lower than that of 3a protein in control 3a transfected 293T cells. In contrast, the full-length 3a protein was readily detected in the culture medium. To directly assess the possible role of each motif for 3a protein release, the tyrosine in YxxΦ motif and the glutamic acid and aspartic acid in diacidic motif were individually substituted with alanine (3aYA and 3aAA, respectively) or in combination (3aA3) (Fig. 6A). All of these 3a mutants were efficiently released from expressing 293T cells (Fig. 6C). These data demonstrated that although the deletion of the 14-aa domain containing the YxxΦ and diacidic acid motifs diminished the release of 3a protein the YxxΦ and diacidic motifs were not directly involved in the release of 3a protein.

DISCUSSION

The present study showed that 3a protein expression alone was sufficient for its release in membrane-bound structures with the buoyant densities of 1.14 to 1.16 g/ml. The release of 3a protein was observed in 293T, Vero E6, and Caco2 cells, indicating it was an intrinsic property of 3a protein. Coronavirus E protein is also known to be released from E protein-expressing cells and infected cells (8, 24). Thus, SCoV 3a protein is the second coronavirus protein that has the ability to be released into culture fluid in the absence of any other viral proteins. Membrane flotation analysis after treatment of 3a-containing membrane structures with 1% Triton-X at room temperature or 4°C implied that the released 3a protein was probably associated with detergent-resistant membranes (5, 7). Further experiments are needed to confirm if 3a protein is associated with lipid rafts by examining the colocalization of 3a protein with the known markers of lipid rafts, such as GM1 or caveoline-1. In addition, the possible role of lipid rafts in the release of 3a also requires further studies. Mutational analysis showed that the YxxΦ and diacidic motifs were not critical for the release of 3a-containing membrane structures. Analysis of supernatants harvested from SCoV-infected cells indicated that 3a protein was most likely released from infected cells in two distinct populations; one, primarily 3a-1, was released as a SCoV structural protein, whereas the other, mostly 3a-2, was released separately in membrane structures of lower densities. Because 3a binds with S protein through disulfide bonds (57) and 3a protein is incorporated into VLP in the cells coexpressing M, E, and 3a protein (43), 3a protein might be incorporated into SCoV particles by interaction with other viral structural proteins in infected cells. The data shown in the present study provide new insights into the biological properties of the SCoV 3a protein.

Several lines of evidence suggested that 3a protein in the culture supernatants of 3a-expressing cells was not merely due to contamination or leaking of the intracellular 3a protein. First of all, there was no overt CPE visible on microscopic examination of the cells. We found that only 3a protein, but not 7a and actin, an abundant intracellular protein, was detected in the culture media of the expressing cells (Fig. 1).

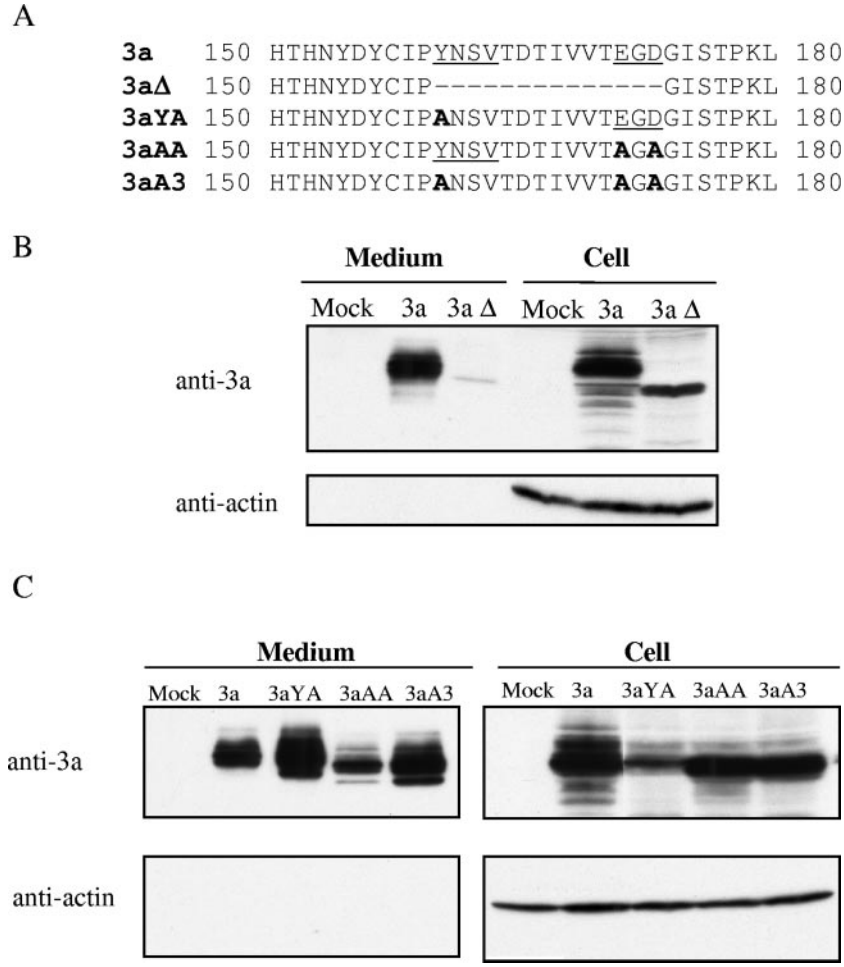

FIG. 6. Role of YxxΦ and diacidic motifs in the release of 3a protein. (A) Partial sequences of the C-terminal region of 3a, 3aΔ, 3aYA, 3aAA, and 3aA3 proteins. YxxΦ and diacidic motifs are underlined. (B and C) 293T cells were independently transfected with pCAGGS (mock), pCAGGS-3a (3a), pCAGGS-3aΔ (3aΔ), pCAGGS-3aYA (3aYA), pCAGGS-3aAA (3aAA), and pCAGGS-3aA3 (3aA3). After 48 h transfection, supernatants from transfected cells were clarified and purified by centrifugation on a 20% sucrose cushion. The pellets were dissolved in 1× SDS-PAGE loading buffer (Medium). Cell lysates were prepared with 1× SDS-PAGE loading buffer (Cell). Samples were subjected to Western blotting analysis with anti-3a antibody to detect 3a protein. The membranes were reprobed with anti-actin antibody (anti-actin).

Additional evidence against the contamination of intracellular 3a protein in the supernatants of 3a-expressing cells was obtained from the analysis of 3aΔ protein. Although the intracellular expression level of 3aΔ protein was comparable with that of wild-type 3a protein, only a trace level of 3aΔ protein was detected in the culture medium of the 3aΔ protein-expressing cells (Fig. 6B). Based on these observations, we concluded that 3a protein detected in the culture supernatants of 3a-expressing cells represented its inherent property to be actively released into the extracellular environment.

Analysis of culture supernatants from SCoV-infected cells with sucrose density equilibrium assay and virus capture assay strongly suggested that 3a-1 was mainly incorporated into SCoV, while some of the 3a-2 was released from SCoV-infected cells in membrane structures with lower densities (Fig. 4 and 5). We did not notice the preferential incorporation of 3a-1 into SCoV in our previous study; our SCoV purification method probably eliminated the membrane structures with lower densities during the procedure (17). The predicted molecular mass of 3a protein is 30.9 kDa (26, 40), indicating that the 3a-1 of 37 kDa underwent certain protein modifications. It has been reported that 3a protein is an O-glycosylated glycoprotein, which is not sensitive to the N-glycosidase enzyme (M. Oostra, C. A. M. de Haan, R. J, de Groot, and P. J. M. Rottier, Xth International Nidovirus Symposium: Toward Control of SARS and Other Nidovirus Disease, abstr. P3-3, 2005). Computational analysis also predicted that 3a protein contains at least five phosphorylation sites for CK1, CK2, and PKA kinases. It is possible that 3a-1, which underwent protein modification, e.g., glycosylation or phosphorylation, was able to efficiently associate with S or M proteins, resulting in preferential incorporation into SCoV.

Our biochemical studies indicated that 3a protein was released in membrane structures from 3a-expressing cells, but we were unable to confirm the presence of 3a protein-associated membrane structures by electron microscopic analysis (data not shown). We observed the presence of heterogeneous particles in the supernatants of 3a-expressing cells by negative

staining. However, we could not confirm the presence of 3a in these vesicles by immunoelectron microscopy using immunogold staining with anti-3a antibody. This result was not unexpected, because the anti-3a antibody recognizes the C-terminal domain of the 3a protein (17), which is most probably not exposed on the exterior of the 3a-containing membrane vesicles. We attempted to probe further by expressing an N-terminal myc-tagged 3a protein; although we could readily detect this protein in supernatants of transfected cells with Western blot assay by using anti-3a antibody, we could not detect the myc tag with potent anti-myc antibodies, either by Western blot analysis of supernatants or immunogold staining of particles. Other researchers have successfully detected a similar myc-tagged 3a protein with anti-myc antibody (47), and we believe the variance in results may be due to cleavage of the N-terminal myc tag during synthesis or lack of accessibility to anti-myc antibody.

Deletion of the region from aa 160 to 173 (160-173 region) containing the YxxΦ and diacidic motifs greatly impaired the release of 3a protein, whereas site-directed mutagenesis analysis of these motifs with alanine substitution indicated that the YxxΦ and diacidic motifs within the 160-173 region were not required for the release of 3a protein. The YxxΦ and diacidic motifs mediate the transport of membrane proteins from the trans-Golgi network to the cell surface (3, 32, 41). The YxxΦ motif serves as a signal for sorting and trafficking proteins to endosomes and lysosomes (4). Equine infectious anemia virus, a member of the retroviruses, uses the YxxL late domain on its Gag protein for virus particle formation by utilizing the host endosomal sorting machinery and the tyrosine is essential for its function (13, 37, 38, 42, 44, 48). We suspect that deletion of the 160-173 region induced a substantial structural alteration in the 3a protein and prevented 3a protein secretion. A possibility emerged that the inability of cell surface translocation of the previously constructed 3a mutant that has the same 160-173 region deletion (47) might be due to a structural alteration of the 3a protein. The clarification of the role of the YxxΦ and di-acidic motifs on cell surface translocation of 3a protein and identification of the 3a protein signal(s) that drove 3a protein release requires further studies.

The biological significance of the release of 3a protein, as well as the presence of 3a protein in virus particles, remains to be determined. During infection, many viruses are capable of releasing viral proteins into the extracellular environment to modulate uninfected cells. For example, human immunodeficiency virus gp120, Tat, and Nef proteins are secreted from infected cells and introduce dramatic changes, including cell death, in bystander cells and uninfected cells (1, 2, 6, 11, 23, 33, 51, 54). The nucleocapsid protein of measles virus is also released from infected cells and induces immunosuppression in neighboring and distant cells (25). It is possible that SCoV might be able to affect neighboring cells or remote cells by secreting 3a protein. In this regard, it is worth noting that 3a protein has been recently reported to cause apoptosis in Vero E6 cells (21).

ACKNOWLEDGMENTS

This study was supported by Public Health Service grant AI29984 to S.M. and contract AI25489 to C.J.P. from the National Institutes of Health. C.H. was supported by the James W. McLaughlin Fellowship Fund, and N.I. was supported by a fellowship for long-term overseas research for young investigators sponsored by the Ministry of Education, Culture, Sports, Science, and Technology of Japan.

REFERENCES

1. **Alimonti, J. B., T. B. Ball, and K. R. Fowke.** 2003. Mechanisms of $CD4^+$ T lymphocyte cell death in human immunodeficiency virus infection and AIDS. J. Gen. Virol. **84:**1649–1661.
2. **Banda, N. K., J. Bernier, D. K. Kurahara, R. Kurrle, N. Haigwood, R. P. Sekaly, and T. H. Finkel.** 1992. Crosslinking CD4 by human immunodeficiency virus gp120 primes T cells for activation-induced apoptosis. J. Exp. Med. **176:**1099–1106.
3. **Bannykh, S. I., N. Nishimura, and W. E. Balch.** 1998. Getting into the Golgi. Trends Cell Biol. **8:**21–25.
4. **Bonifacino, J. S., and L. M. Traub.** 2003. Signals for sorting of transmembrane proteins to endosomes and lysosomes. Annu. Rev. Biochem. **72:**395–447.
5. **Briggs, J. A., T. Wilk, and S. D. Fuller.** 2003. Do lipid rafts mediate virus assembly and pseudotyping? J. Gen. Virol. **84:**757–768.
6. **Chang, H. C., F. Samaniego, B. C. Nair, L. Buonaguro, and B. Ensoli.** 1997. HIV-1 Tat protein exits from cells via a leaderless secretory pathway and binds to extracellular matrix-associated heparan sulfate proteoglycans through its basic region. AIDS **11:**1421–1431.
7. **Chazal, N., and D. Gerlier.** 2003. Virus entry, assembly, budding, and membrane rafts. Microbiol. Mol. Biol. Rev. **67**:226–237.
8. **Corse, E., and C. E. Machamer.** 2000. Infectious bronchitis virus E protein is targeted to the Golgi complex and directs release of virus-like particles. J. Virol. **74:**4319–4326.
9. **de Haan, C. A., P. S. Masters, X. Shen, S. Weiss, and P. J. Rottier.** 2002. The group-specific murine coronavirus genes are not essential, but their deletion, by reverse genetics, is attenuating in the natural host. Virology **296:**177–189.
10. **Drosten, C., S. Gunther, W. Preiser, S. van der Werf, H. R. Brodt, S. Becker, H. Rabenau, M. Panning, L. Kolesnikova, R. A. Fouchier, A. Berger, A. M. Burguiere, J. Cinatl, M. Eickmann, N. Escriou, K. Grywna, S. Kramme, J. C. Manuguerra, S. Muller, V. Rickerts, M. Sturmer, S. Vieth, H. D. Klenk, A. D. Osterhaus, H. Schmitz, and H. W. Doerr.** 2003. Identification of a novel coronavirus in patients with severe acute respiratory syndrome. N. Engl. J. Med. **348:**1967–1976.
11. **Ensoli, B., G. Barillari, S. Z. Salahuddin, R. C. Gallo, and F. Wong-Staal.** 1990. Tat protein of HIV-1 stimulates growth of cells derived from Kaposi's sarcoma lesions of AIDS patients. Nature **345:**84–86.
12. **Fielding, B. C., Y. J. Tan, S. Shuo, T. H. Tan, E. E. Ooi, S. G. Lim, W. Hong, and P. Y. Goh.** 2004. Characterization of a unique group-specific protein (U122) of the severe acute respiratory syndrome coronavirus. J. Virol. **78:** 7311–7318.
13. **Freed, E. O.** 2002. Viral late domains. J. Virol. **76:**4679–4687.
14. **Goldsmith, C. S., K. M. Tatti, T. G. Ksiazek, P. E. Rollin, J. A. Comer, W. W. Lee, P. A. Rota, B. Bankamp, W. J. Bellini, and S. R. Zaki.** 2004. Ultrastructural characterization of SARS coronavirus. Emerg. Infect. Dis. **10:**320–326.
15. **Ho, Y., P. H. Lin, C. Y. Liu, S. P. Lee, and Y. C. Chao.** 2004. Assembly of human severe acute respiratory syndrome coronavirus-like particles. Biochem. Biophys. Res. Commun. **318:**833–838.
16. **Huang, Y., Z. Y. Yang, W. P. Kong, and G. J. Nabel.** 2004. Generation of synthetic severe acute respiratory syndrome coronavirus pseudoparticles: implications for assembly and vaccine production. J. Virol. **78:**12557–12565.
17. **Ito, N., E. C. Mossel, K. Narayanan, V. L. Popov, C. Huang, T. Inoue, C. J. Peters, and S. Makino.** 2005. Severe acute respiratory syndrome coronavirus 3a protein is a viral structural protein. J. Virol. **79:**3182–3186.
18. **Ksiazek, T. G., D. Erdman, C. S. Goldsmith, S. R. Zaki, T. Peret, S. Emery, S. Tong, C. Urbani, J. A. Comer, W. Lim, P. E. Rollin, S. F. Dowell, A. E. Ling, C. D. Humphrey, W. J. Shieh, J. Guarner, C. D. Paddock, P. Rota, B. Fields, J. DeRisi, J. Y. Yang, N. Cox, J. M. Hughes, J. W. LeDuc, W. J. Bellini, and L. J. Anderson.** 2003. A novel coronavirus associated with severe acute respiratory syndrome. N. Engl. J. Med. **348:**1953–1966.
19. **Kuiken, T., R. A. Fouchier, M. Schutten, G. F. Rimmelzwaan, G. van Amerongen, D. van Riel, J. D. Laman, T. de Jong, G. van Doornum, W. Lim, A. E. Ling, P. K. Chan, J. S. Tam, M. C. Zambon, R. Gopal, C. Drosten, S. van der Werf, N. Escriou, J. C. Manuguerra, K. Stohr, J. S. Peiris, and A. D. Osterhaus.** 2003. Newly discovered coronavirus as the primary cause of severe acute respiratory syndrome. Lancet **362:**263–270.
20. **Lai, M. M. C., and K. V. Holmes.** 2001. Coronaviruses, p. 1163–1185. *In* D. M. Knipe and P. M. Howley (ed.), Fields virology, 4th ed. Lippincott, Philadelphia, Pa.
21. **Law, P. T., C. H. Wong, T. C. Au, C. P. Chuck, S. K. Kong, P. K. Chan, K. F. To, A. W. Lo, J. Y. Chan, Y. K. Suen, H. Y. Chan, K. P. Fung, M. M. Waye, J. J. Sung, Y. M. Lo, and S. K. Tsui.** 2005. The 3a protein of severe acute respiratory syndrome-associated coronavirus induces apoptosis in Vero E6 cells. J. Gen. Virol. **86:**1921–1930.
22. **Lee, N., D. Hui, A. Wu, P. Chan, P. Cameron, G. M. Joynt, A. Ahuja, M. Y. Yung, C. B. Leung, K. F. To, S. F. Lui, C. C. Szeto, S. Chung, and J. J. Sung.** 2003. A major outbreak of severe acute respiratory syndrome in Hong Kong. N. Engl. J. Med. **348:**1986–1994.

23. **Li, C. J., D. J. Friedman, C. Wang, V. Metelev, and A. B. Pardee.** 1995. Induction of apoptosis in uninfected lymphocytes by HIV-1 Tat protein. Science **268:**429–431.
24. **Maeda, J., A. Maeda, and S. Makino.** 1999. Release of coronavirus E protein in membrane vesicles from virus-infected cells and E protein-expressing cells. Virology **263:**265–272.
25. **Marie, J. C., F. Saltel, J. M. Escola, P. Jurdic, T. F. Wild, and B. Horvat.** 2004. Cell surface delivery of the measles virus nucleoprotein: a viral strategy to induce immunosuppression. J. Virol. **78:**11952–11961.
26. **Marra, M. A., S. J. Jones, C. R. Astell, R. A. Holt, A. Brooks-Wilson, Y. S. Butterfield, J. Khattra, J. K. Asano, S. A. Barber, S. Y. Chan, A. Cloutier, S. M. Coughlin, D. Freeman, N. Girn, O. L. Griffith, S. R. Leach, M. Mayo, H. McDonald, S. B. Montgomery, P. K. Pandoh, A. S. Petrescu, A. G. Robertson, J. E. Schein, A. Siddiqui, D. E. Smailus, J. M. Stott, G. S. Yang, F. Plummer, A. Andonov, H. Artsob, N. Bastien, K. Bernard, T. F. Booth, D. Bowness, M. Czub, M. Drebot, L. Fernando, R. Flick, M. Garbutt, M. Gray, A. Grolla, S. Jones, H. Feldmann, A. Meyers, A. Kabani, Y. Li, S. Normand, U. Stroher, G. A. Tipples, S. Tyler, R. Vogrig, D. Ward, B. Watson, R. C. Brunham, M. Krajden, M. Petric, D. M. Skowronski, C. Upton, and R. L. Roper.** 2003. The genome sequence of the SARS-associated coronavirus. Science **300:**1399–1404.
27. **Mortola, E., and P. Roy.** 2004. Efficient assembly and release of SARS coronavirus-like particles by a heterologous expression system. FEBS Lett. **576:**174–178.
28. **Mossel, E. C., C. Huang, K. Narayanan, S. Makino, R. B. Tesh, and C. J. Peters.** 2005. Exogenous ACE2 expression allows refractory cell lines to support severe acute respiratory syndrome coronavirus replication. J. Virol. **79:**3846–3850.
29. **Narayanan, K., A. Maeda, J. Maeda, and S. Makino.** 2000. Characterization of the coronavirus M protein and nucleocapsid interaction in infected cells. J. Virol. **74:**8127–8134.
30. **Nelson, C. A., A. Pekosz, C. A. Lee, M. S. Diamond, and D. H. Fremont.** 2005. Structure and intracellular targeting of the SARS-coronavirus Orf7a accessory protein. Structure **13:**75–85.
31. **Nguyen, D. G., A. Booth, S. J. Gould, and J. E. Hildreth.** 2003. Evidence that HIV budding in primary macrophages occurs through the exosome release pathway. J. Biol. Chem. **278:**52347–52354.
32. **Nishimura, N., H. Plutner, K. Hahn, and W. E. Balch.** 2002. The delta subunit of AP-3 is required for efficient transport of VSV-G from the trans-Golgi network to the cell surface. Proc. Natl. Acad. Sci. USA **99:**6755–6760.
33. **Okada, H., R. Takei, and M. Tashiro.** 1997. HIV-1 Nef protein-induced apoptotic cytolysis of a broad spectrum of uninfected human blood cells independently of CD95(Fas). FEBS Lett. **414:**603–606.
34. **Ortego, J., I. Sola, F. Almazan, J. E. Ceriani, C. Riquelme, M. Balasch, J. Plana, and L. Enjuanes.** 2003. Transmissible gastroenteritis coronavirus gene 7 is not essential but influences in vivo virus replication and virulence. Virology **308:**13–22.
35. **Paul, P. S., E. M. Vaughn, and P. G. Halbur.** 1997. Pathogenicity and sequence analysis studies suggest potential role of gene 3 in virulence of swine enteric and respiratory coronaviruses. Adv. Exp. Med. Biol. **412:**317–321.
36. **Peiris, J. S., S. T. Lai, L. L. Poon, Y. Guan, L. Y. Yam, W. Lim, J. Nicholls, W. K. Yee, W. W. Yan, M. T. Cheung, V. C. Cheng, K. H. Chan, D. N. Tsang, R. W. Yung, T. K. Ng, and K. Y. Yuen.** 2003. Coronavirus as a possible cause of severe acute respiratory syndrome. Lancet **361:**1319–1325.
37. **Pornillos, O., J. E. Garrus, and W. I. Sundquist.** 2002. Mechanisms of enveloped RNA virus budding. Trends Cell Biol. **12:**569–579.
38. **Puffer, B. A., L. J. Parent, J. W. Wills, and R. C. Montelaro.** 1997. Equine infectious anemia virus utilizes a YXXL motif within the late assembly domain of the Gag p9 protein. J. Virol. **71:**6541–6546.
39. **Qinfen, Z., C. Jinming, H. Xiaojun, Z. Huanying, H. Jicheng, F. Ling, L. Kunpeng, and Z. Jingqiang.** 2004. The life cycle of SARS coronavirus in Vero E6 cells. J. Med. Virol. **73:**332–337.
40. **Rota, P. A., M. S. Oberste, S. S. Monroe, W. A. Nix, R. Campagnoli, J. P. Icenogle, S. Penaranda, B. Bankamp, K. Maher, M. H. Chen, S. Tong, A. Tamin, L. Lowe, M. Frace, J. L. DeRisi, Q. Chen, D. Wang, D. D. Erdman, T. C. Peret, C. Burns, T. G. Ksiazek, P. E. Rollin, A. Sanchez, S. Liffick, B. Holloway, J. Limor, K. McCaustland, M. Olsen-Rasmussen, R. Fouchier, S. Gunther, A. D. Osterhaus, C. Drosten, M. A. Pallansch, L. J. Anderson, and W. J. Bellini.** 2003. Characterization of a novel coronavirus associated with severe acute respiratory syndrome. Science **300:**1394–1399.
41. **Sevier, C. S., O. A. Weisz, M. Davis, and C. E. Machamer.** 2000. Efficient export of the vesicular stomatitis virus G protein from the endoplasmic reticulum requires a signal in the cytoplasmic tail that includes both tyrosine-based and di-acidic motifs. Mol. Biol. Cell **11:**13–22.
42. **Shehu-Xhilaga, M., S. Ablan, D. G. Demirov, C. Chen, R. C. Montelaro, and E. O. Freed.** 2004. Late domain-dependent inhibition of equine infectious anemia virus budding. J. Virol. **78:**724–732.
43. **Shen, S., P. S. Lin, Y. C. Chao, A. Zhang, X. Yang, S. G. Lim, W. Hong, and Y. J. Tan.** 2005. The severe acute respiratory syndrome coronavirus 3a is a novel structural protein. Biochem. Biophys. Res. Commun. **330:**286–292.
44. **Strack, B., A. Calistri, S. Craig, E. Popova, and H. G. Gottlinger.** 2003. AIP1/ALIX is a binding partner for HIV-1 p6 and EIAV p9 functioning in virus budding. Cell **114:**689–699.
45. **Tan, Y. J., B. C. Fielding, P. Y. Goh, S. Shen, T. H. Tan, S. G. Lim, and W. Hong.** 2004. Overexpression of 7a, a protein specifically encoded by the severe acute respiratory syndrome coronavirus, induces apoptosis via a caspase-dependent pathway. J. Virol. **78:**14043–14047.
46. **Tan, Y. J., P. Y. Goh, B. C. Fielding, S. Shen, C. F. Chou, J. L. Fu, H. N. Leong, Y. S. Leo, E. E. Ooi, A. E. Ling, S. G. Lim, and W. Hong.** 2004. Profiles of antibody responses against severe acute respiratory syndrome coronavirus recombinant proteins and their potential use as diagnostic markers. Clin. Diagn. Lab. Immunol. **11:**362–371.
47. **Tan, Y. J., E. Teng, S. Shen, T. H. Tan, P. Y. Goh, B. C. Fielding, E. E. Ooi, H. C. Tan, S. G. Lim, and W. Hong.** 2004. A novel severe acute respiratory syndrome coronavirus protein, u274, is transported to the cell surface and undergoes endocytosis. J. Virol. **78:**6723–6734.
48. **Tanzi, G. O., A. J. Piefer, and P. Bates.** 2003. Equine infectious anemia virus utilizes host vesicular protein sorting machinery during particle release. J. Virol. **77:**8440–8447.
49. **Thiel, V., K. A. Ivanov, A. Putics, T. Hertzig, B. Schelle, S. Bayer, B. Weissbrich, E. J. Snijder, H. Rabenau, H. W. Doerr, A. E. Gorbalenya, and J. Ziebuhr.** 2003. Mechanisms and enzymes involved in SARS coronavirus genome expression. J. Gen. Virol. **84:**2305–2315.
50. **Tooze, J., S. A. Tooze, and S. D. Fuller.** 1987. Sorting of progeny coronavirus from condensed secretory proteins at the exit from the trans-Golgi network of AtT20 cells. J. Cell Biol. **105:**1215–1226.
51. **Trillo-Pazos, G., E. McFarlane-Abdulla, I. C. Campbell, G. J. Pilkington, and I. P. Everall.** 2000. Recombinant nef HIV-IIIB protein is toxic to human neurons in culture. Brain Res. **864:**315–326.
52. **Vaughn, E. M., P. G. Halbur, and P. S. Paul.** 1995. Sequence comparison of porcine respiratory coronavirus isolates reveals heterogeneity in the S, 3, and 3–1 genes. J. Virol. **69:**3176–3184.
53. **Wesley, R. D., R. D. Woods, and A. K. Cheung.** 1991. Genetic analysis of porcine respiratory coronavirus, an attenuated variant of transmissible gastroenteritis virus. J. Virol. **65:**3369–3373.
54. **Westendorp, M. O., R. Frank, C. Ochsenbauer, K. Stricker, J. Dhein, H. Walczak, K. M. Debatin, and P. H. Krammer.** 1995. Sensitization of T cells to CD95-mediated apoptosis by HIV-1 Tat and gp120. Nature **375:**497–500.
55. **Yu, C. J., Y. C. Chen, C. H. Hsiao, T. C. Kuo, S. C. Chang, C. Y. Lu, W. C. Wei, C. H. Lee, L. M. Huang, M. F. Chang, H. N. Ho, and F. J. Lee.** 2004. Identification of a novel protein 3a from severe acute respiratory syndrome coronavirus. FEBS Lett. **565:**111–116.
56. **Yuan, X., J. Li, Y. Shan, Z. Yang, Z. Zhao, B. Chen, Z. Yao, B. Dong, S. Wang, J. Chen, and Y. Cong.** 2005. Subcellular localization and membrane association of SARS-CoV 3a protein. Virus Res. **109:**191–202.
57. **Zeng, R., R. F. Yang, M. D. Shi, M. R. Jiang, Y. H. Xie, H. Q. Ruan, X. S. Jiang, L. Shi, H. Zhou, L. Zhang, X. D. Wu, Y. Lin, Y. Y. Ji, L. Xiong, Y. Jin, E. H. Dai, X. Y. Wang, B. Y. Si, J. Wang, H. X. Wang, C. E. Wang, Y. H. Gan, Y. C. Li, J. T. Cao, J. P. Zuo, S. F. Shan, E. Xie, S. H. Chen, Z. Q. Jiang, X. Zhang, Y. Wang, G. Pei, B. Sun, and J. R. Wu.** 2004. Characterization of the 3a protein of SARS-associated coronavirus in infected Vero E6 cells and SARS patients. J. Mol. Biol. **341:**271–279.